

# CAP-DSDN: Node Co-association Prediction in Communities in Dynamic Sparse Directed Networks and a Case Study of Migration Flow

Jaya Sreevalsan-Nair<sup>1</sup> <sup>a</sup> and Astha Jakher<sup>2</sup>

<sup>1</sup>Graphics-Visualization-Computing Lab, International Institute of Information Technology Bangalore, Bangalore, India

<sup>2</sup>Department of Humanities and Social Sciences, IIT Kharagpur, Kharagpur, West Bengal 721302, India

**Keywords:** Real-world Graphs, Directed Networks, Edge Sparsity, Dynamic Networks, Community Detection, Community Evaluation, Migration Flows, Co-association, Prediction, Autoregressive Models, VAR Model, ARMA Model.


**Abstract:** Predicting the community structure in the time series, or *snapshots*, of a real-world graph in the future, is a pertinent challenge. This is motivated by the study of migration flow networks. The dataset is characterized by edge sparsity due to the inconsistent availability of data. Thus, we generalize the problem to predicting community structure in a dynamic sparse directed network (DSDN). We introduce a novel application of *co-association* which is a pairwise relationship between the nodes belonging to the same community. We thus propose a three-step algorithm, CAP-DSDN, for co-association prediction (CAP) in such a network. Given the absence of benchmark data or ground truth, we use an ensemble of community detection (CD) algorithms and evaluation metrics widely used for directed networks. We then define a metric based on entropy rate as a threshold to filter the network for determining a significant and data-complete subnetwork. We propose the use of autoregressive models for predicting the co-association relationship given in its matrix format. We demonstrate the effectiveness of our proposed method in a case study of international refugee migration during 2000–18. Our results show that our method works effectively for migration flow networks for short-term prediction and when the data is complete across all snapshots.

## 1 INTRODUCTION

The communities in the time series of directed networks (Malliaros and Vazirgiannis, 2013) enable us to understand the change in the network topology in real-world graphs. Let us take the example of the international refugee migration network. Using the migration flow data for  $n$  consecutive years, referred to as *snapshots*, we get the time series of a directed network, where the countries are nodes and the migrant counts are the edge weights. Predicting a network at a future time is difficult as it involves predicting the occurrence of edges, *i.e.*, pairwise relationship between nodes, and their weights. This issue deteriorates in the case of edge-sparse networks where there is no specific known model for the occurrence of edges. For instance, in the case of migration networks, there are socio-economic-political systemic dependencies, natural disasters, and other factors for the additions and deletions of nodes and edges in the network which are often complex to predict (Suleimenova et al., 2017).

At the same time, the data is not consistently available for any given pair of countries owing to lapses in data curation and communication (Neumayer, 2005). This inconsistency in the availability of edge data also leads to inaccuracy in the study of network community structures. Hence, we shift our focus to studying the community behavior of nodes in the network instead of the communities themselves. Thus, we focus on using the *persistent community behavior* of nodes in the time series to predict its community behavior in the future. We propose an algorithm, CAP-DSDN<sup>1</sup> (Co-Association Prediction in Dynamic Sparse Directed Network), for predicting the *co-association between nodes* in the  $(n+1)^{\text{th}}$  year, using the data until the  $n^{\text{th}}$  year.

As an example, if the United States of America (USA) and Mexico *co-existed* in a community over most part of the  $n$ -year period, can we then use the available data to predict their co-association in a community, *i.e.*, membership to the same community, in the  $(n+1)^{\text{th}}$  year? Our proposed algorithm, CAP-

<sup>a</sup>  <https://orcid.org/0000-0001-6333-4161>

<sup>1</sup>Pronounced as  $\backslash kap-duhs-durn \backslash$ .

DSDN (Figure 1) predicts such co-associations at a future time instance, which in turn helps in inferring the community structure. It must be noted that CAP-DSDN does not predict the number of communities or their constituencies. Instead, CAP-DSDN predicts the likelihood of any two nodes being in the same community in the future.

Our novel contributions towards community analysis in DSDNs are:

- A three-step algorithm, CAP-DSDN, for co-association prediction (CAP) for implicitly forecasting community behavior in real-world graphs which are DSDNs.
- Definition of a metric of entropy rate  $H$  to be used on the co-association matrices (CAM) for determining persistent community behavior of the nodes, and thus, a threshold  $\tau_h$  for node-filtering the network to address the issue of sparsity.
- A method of applying time series autoregressive models to CAMs.

## 2 RELATED WORK

Recently, the communities in DSDNs have been modeled as routed activity-driven networks for modeling its community structure (Bongiorno et al., 2019). Here, starting from a set of existing community detection (CD) algorithms, such as Louvain, Infomap, etc., the communities are improved by using the proposed characterization. A recent study on the state-of-the-art CD algorithms for dynamic networks has shown that the choice of algorithm is contextual and is based on the nature of communities and community events involved in such networks (Rossetti and Cazabet, 2018).

In the classification of different CD algorithms (Rossetti and Cazabet, 2018), CAP-DSDN falls in the category of *instant optimal CD* approach that finds communities in each snapshot and matches communities across snapshots. A known disadvantage of this approach is that it is ambiguous if the evolution in community structures is due to the actual evolution of events or due to the instabilities of CD algorithms in each timestamp.

There has been an empirical comparison of CD algorithms for directed networks (Agreste et al., 2016), which has studied the accuracy and time complexity of selected state-of-the-art methods on real and synthetic datasets. This work has concluded that the WalkTrap algorithm (Pons and Latapy, 2006) has the highest accuracy, but the worst time complexity. The other key algorithms discussed in this

work are Infomap (IMAP) (Rosvall and Bergstrom, 2008), eigenvector algorithm or the modularity optimization for directed networks (MODN) (Leicht and Newman, 2008), and speaker-listener label propagation algorithm (SLPA) (Xie et al., 2011). The algorithms are further classified as follows, based on how they use the directionality information of the networks: (i) directionality-preserving ones, e.g., Infomap and label propagation algorithm, and (ii) directionality-discarding ones, e.g., eigenvector algorithm and WalkTrap.

SLPA is based on directional propagation of labels, whereas MODN defines a community based on high and low densities of intra- and inter-community edges, respectively; and IMAP uses random walks to determine communities. Thus, these methods fall in different categories of models used for CD, namely, models based on *dynamic processes on graphs*, on a *null model*, and on a *flow model*, respectively (Agreste et al., 2016). SLPA and IMAP are efficient methods and scalable to large graphs (Agreste et al., 2016). SLPA and IMAP methods use the directionality information, whereas MODN ignores the same by using a symmetric adjacency matrix.

- **Speaker Listener Label Propagation Algorithm (SLPA)** (Xie et al., 2011): is an extension of the label propagation algorithm which initially assigns each node with a unique label and iteratively updates labels to the most frequently occurring label in the neighborhood of the node. SLPA extends to overlapping communities, where nodes can have multiple labels based on their role as a listener or a speaker.
- **Modularity Optimization for Directed Networks (MODN) Algorithm** (Leicht and Newman, 2008): uses the variant of Girvan-Newman modularity for directed networks, given by:

$$Q = \frac{1}{2m} \sum_{i,j} [A_{i,j} - \frac{k_i k_j}{2m}] \delta(C_i, C_j),$$

where  $A_{ij}$  is an element of the adjacency matrix  $A$  giving edge weight between nodes  $i$  and  $j$ ,  $\delta_{ij}$  is the Kronecker delta,  $C_i$  is the label of the community to which node  $i$  belongs,  $k_i$  is the degree of node  $i$ , and  $2m$  is the sum of degrees of all nodes in the network. The algorithm is implemented as an optimization problem, where  $Q$  is maximized for community detection. The maximum value of  $Q$  is considered as the best approximation of the true communities in the network.

- **Infomap (IMAP) Algorithm** (Rosvall and Bergstrom, 2008): is based on information theory, using the map equation. The entropy of random walks within and between modules

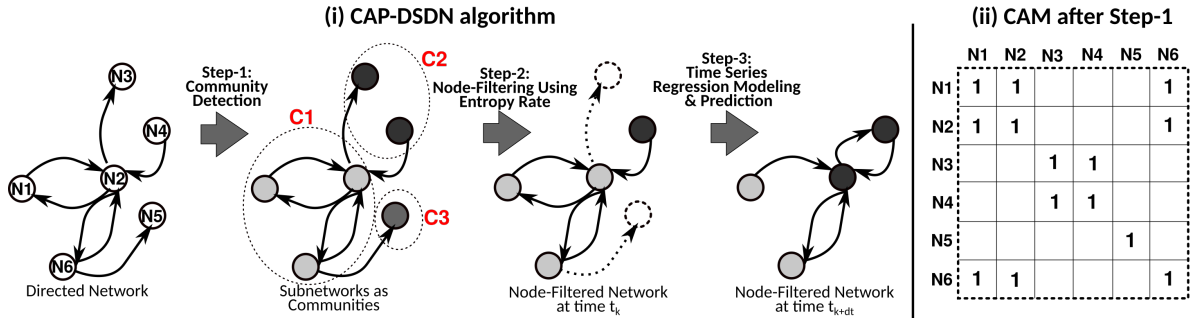


Figure 1: (i) Our proposed three-step algorithm, CAP-DSDN, for prediction of community behavior of nodes in a dynamic sparse directed network (DSDN), where the node color indicates community ID. (ii) The co-association matrix (CAM) of the network after community detection (CD) in Step-1.

is used in a cost function in the map equation. This cost function is the expected description length of a random walk, which is minimized. Thus, the best node-partitioning occurs where the probability flow is the most cost-efficient.

Community detection has been recently implemented on sparse directed networks using a parameter-Sparse Random Graph Model, that preserves the directionality (Stein and Leng, 2021). This involves modeling using an estimator using an  $l_1$  penalty to achieve sparsity in parameter space to simulate a sparse network. Previously, spectral methods have been used extensively for sparse directed networks using the spectrum of the non-backtracking matrix (Singh and Humphries, 2015; Krzakala et al., 2013). Spectral methods using non- and reluctant-backtracking matrices have been successfully used for real-world graphs (Singh and Humphries, 2015).

Perturbing and resampling network has been done to aggregate information in large sparse undirected networks (Mirshahvalad et al., 2012). This is similar to our proposed method of using an information-theoretic metric of entropy rate for assessing the statistical significance of communities. The size of a controllable subnetwork for a node has been used to determine the statistical significance of the node in sparse directed networks (Wang et al., 2012). This is similar to how we use moving average smoothing for finding significant nodes.

There is limited work on community detection in dynamic sparse directed networks (DSDNs). Recently, a consensus method has been used to determine the state of clusters of nodes (Martin et al., 2016). The rationale for tracking the state of the node clusters is for reducing the dimensionality of DSDNs. Our work is different, as we are focused on predicting co-association values, so as to not limit our analysis to the raw network data alone.

### 3 PRELIMINARIES

Here, we define the Co-association Matrix (CAM) and persistent community behavior.

**Definition 1.** A *Co-association Matrix (CAM)* is a symmetric matrix with rows and columns representing the same set of data items, say countries in the migration flow network, in the same order, and each cell  $(i, j)$  indicates if the item in the  $i^{\text{th}}$  row and that in the  $j^{\text{th}}$  column are associated with the same cluster, i.e., belong to the same community in the case of networks.

**Definition 2.** *Persistent Community Behavior* is a property of a node of a dynamic network where it has a high likelihood of non-zero co-association with other nodes in a network across several snapshots.

### 4 CAP-DSDN: OUR PROPOSED METHOD

Our three-step algorithm, CAP-DSDN, is as follows: **Step-1:** Perform community detection in each snapshot of a DSDN using an ensemble of CD algorithms and compute an aggregated CAM.

**Step-2:** Determine a subnetwork of nodes with persistent community behavior using the aggregated CAM, thus implementing node-filtering the network.

**Step-3:** Perform time series autoregressive models on the CAM of the filtered network to predict the community structure in the subnetwork in the future.

To handle the limitations of analysis stemming from the sparsity in the networks, our approach is to localize our analysis to a subnetwork that shows *persistent* community behavior. Thus, we further analyze a relatively denser subnetwork, which is determined using the preprocessing steps **Step-1** and **Step-2**. The

requirement of a dense network also comes from the insufficiency of data for a prediction algorithm.

We predict the co-association between nodes of the network instead of the edge weight as the co-association value has the property of being bounded between 0 and 1, unlike the edge weight. The predicted co-association value is the probability or likelihood of two nodes belonging to the same community in the future using their past behavior. Since the community behavior is computed independently in each snapshot with the information from the neighboring snapshots, we now use the concept of *moving average* to compute the probability of co-association using a shorter time window, e.g., five snapshots, as explained in Section 4.1.

We also do not pursue the idea of predicting the likelihood of the occurrence of an edge in this work, as the networks of interest are weighted networks and not binary ones.

#### 4.1 Step-1: Community Detection

In this step, we compute a CAM for each snapshot of the network. The inputs to this step are a DSDN and a CD algorithm, and the outputs are a time series of community IDs for the nodes.

A community structure selected from an ensemble of methods based on its performance is a reliable choice in the absence of ground truth in real-world graphs. Thus, the crux of this step is in identifying an appropriate CD algorithm for DSDNs. Based on a literature survey on widely used algorithms for CD in directed networks (Agrete et al., 2016), we have selected three algorithms, namely, Speaker-Listener Label Propagation Algorithm (SLPA), modularity optimization for directed networks (MODN), and Infomap algorithm (IMAP). These algorithms are designed using different approaches, as explained in Section 2, which make them suitable for comparative analysis in our work.

**Choice of CD Algorithm:** We choose a CD algorithm for a DSDN using the following strategies:

- *Community Quality Metrics:* We compute the quality of node-partitioning to form communities using selected community quality metrics. We then consider an algorithm to be *better performing* when its outcomes are closer to the best quality.
- *Characteristics of CD Outcomes in the Time Series:* We consider an algorithm to be *better performing* if it has consistently created more than one community across snapshots. An algorithm that leads to under- or over-fragmentation is not preferred, which avoids scenarios of monolithic and overly fragmented communities, respectively.

We identify widely used metrics using a literature survey and use the following six metrics in this work, namely, link modularity (LM) (Nicosia et al., 2009), internal edge density (IED) (Radicchi et al., 2004), average internal degree (AID) (Radicchi et al., 2004), cut ratio (CR) (Fortunato, 2010), and Z-modularity (ZM) (Miyachi and Kawase, 2016). It is important to use appropriate metrics for validation, given the absence of benchmark datasets with ground truth in real-world graphs. Hence, the final set is identified based on the better performance of the CD algorithm on these metrics for our case study.

**Computing CAMs:** The CAM captures the tendency of any two given nodes belonging to the same community/cluster/node-grouping. The co-association relationship between nodes  $i$  and  $j$  belonging to communities  $C_i$  and  $C_j$ , respectively, at time instance  $T$ , is captured in the following matrix element in CAM:

$$D_{ij}(T) = \begin{cases} 1 & , \text{ if } (C_i(T) = C_j(T)) \text{ and } (i \neq j), \\ 0 & , \text{ otherwise.} \end{cases} \quad (1)$$

**Probability of Co-association Matrices (PCAMs):**

For incorporating the temporal context, CAMs of consecutive snapshots can now be averaged to obtain a probability matrix (or transition matrix), thus, giving the likelihood of each pair of nodes belonging to the same community for those years. We refer to this matrix as the *probability of co-association matrix* (PCAM), which is computed by averaging the CAMs in the moving time-window  $\Delta_T$ , and hence referred to as  $P(T, \Delta_T)$ . Thus, the probability of co-association between nodes  $i$  and  $j$  at time instance  $T$ , using values backward in time, is:

$$P_{ij}(T, \Delta_T) = \frac{1}{\Delta_T} \sum_{t=T-\Delta_T+1}^T D_{ij}(t). \quad (2)$$

Thus, CAM has binary values ‘0’ and ‘1’, and PCAM has real values in  $[0,1]$ . We further use the PCAMs for the prediction model in Step-3 (Section 4.3).

#### 4.2 Step-2: Node-filtering the Network

Given the quadratic complexity of CAM with an attribute set of size  $N_a$ , we observe that ( $N_a \gg N_T$ ), for  $N_T$  time instances in real-world graphs. Hence, any time series analysis runs into the risk of *over-fitting*. Thus, given the edge sparsity of the network, there is a requirement to reduce  $N_a$ . We achieve this by retaining the *significant* nodes with highly persistent community behavior. Such nodes demonstrate a high tendency to be part of a *sufficiently* large community through most of the period of interest. We pay attention to the size of the communities to which these

nodes belong so that we filter out overly fragmented *i.e.*, small communities. We choose *node-filtering* over *edge-filtering* here because, though the filtering occurs in the CAM which represents relationships between nodes, it must also be simultaneously applied to the original directed network. CAM is equivalent to an undirected co-association network but uses the same node-set as the original network. Thus, we filter the nodes instead of the edges to simultaneously apply it on both the CAM and the original DSDN.

#### Defining a Metric for Threshold: Entropy Rate:

The *persistence* of the co-associations in a network gives the temporal significance of the relationship between nodes, which is computed using the time series of the probability values in PCAMs. Here, we are interested in the temporal significance of the nodes to decide if the node is to be filtered out or retained. Hence, we compute the significance of the node using the persistence of its co-associations in the network.

To compute the node-wise significance, we first average the PCAMs over a specific period and then average across either the rows or the columns, since it is a symmetric matrix. Thus, for each node  $i$  in a network of  $n$  nodes, its probability of associating with other nodes in the window of time  $(T - \Delta_T, T]$ , is:

$$p_i(T, \Delta_T) = \frac{1}{(n-1)} \cdot \sum_{j=1}^n P_{ij}(T, \Delta_T). \quad (3)$$

We use the averaging operator here instead of other statistical operators, as the average gives us a likelihood or probability value. We can now also see that for each node  $i$ , the  $(N_T - \Delta_T + 1)$  instances of these probability values is effectively the *moving average smoothing* of the degree of the node in the CAM, for a window of size  $\Delta_T$ . Hence, this operation is a *moving average of order  $\Delta_T$  or  $\Delta_T$ -MA*.

The  $\Delta_T$ -MA sequence is derived from a time series, and hence, is a *stochastic process*, by design. The time series of edge weights of a real-world graph is a stationary process (Cai et al., 2016), and hence the  $\Delta_T$ -MA sequence of PCAM elements is also a stationary process. For a stochastic process of  $n$  random variables, its *entropy rate* gives us a measure of how the entropy of the sequence grows with  $n$  (Cover and Thomas, 2006). In our case, the entropy rate of the sequence of probability values at each node gives us the change in the tendency of the node to co-associate with other nodes in communities.

The entropy rate of the stochastic process  $X$  is given by the limiting value of the joint entropy of the  $m$  members of the process  $\{X_1, X_2, \dots, X_m\}$ :

$$H(X) = \lim_{m \rightarrow \infty} \frac{1}{m} H(X_1, X_2, \dots, X_m)$$

For a discrete case of joint entropy, the joint entropy of a set of random variables is bounded by the

sum of entropy of the individual variables (Cover and Thomas, 2006):

$$H(X_1, X_2, \dots, X_m) \leq \sum_{i=1}^m H(X_i) = \sum_{i=1}^m (-p_i \log(p_i)).$$

Thus, we get the upper bound of entropy rate at each node  $i$ , for time sequence  $(t_1, \dots, t_{\Delta_T}, \dots, t_{N_T})$  as a function of window size  $\Delta_T$  for moving average smoothing:

$$H_i(\Delta_T) = \sum_{k=\Delta_T}^{N_T} -(p_i(t_k, \Delta_T) \log(p_i(t_k, \Delta_T))). \quad (4)$$

**Choice of Threshold for Node-filtering:** We observe that the entropy rate of a node  $i$ ,  $H_i$ , is closer to 0 when the node is highly likely to co-associate with other nodes, *i.e.*,  $p_i(t_k, \Delta_T) \approx 1$  across all snapshots. Thus, the entropy rate for a node  $H_i$  is *inversely proportional* to the *likelihood* of its persistent community behavior. Hence, we identify a threshold for  $H_i$ , where nodes with an entropy rate higher than the threshold are filtered out.

We propose to determine the threshold,  $\tau_h$ , using a line plot of sorted entropy rates of all the nodes in the network and the size of the node-filtered network. A steep increase in the entropy rate at a transition point  $\tau_h$  implies that the network maintains low entropy until this point. We observe that the real-world graph tends to have two groups of nodes that correspond to low and high entropy rates, where the presence of any node from the latter tends to sharply increase the size of the node-filtered network.

In the node-filtered network of  $n'$  nodes, we now have  $N'_a = \frac{n'(n'-1)}{2}$  attributes. Since  $(N'_a < N_a)$ , we reasonably reduce the gap between  $N'_a$  and  $N_T$ , even though  $(N'_a \gg N_T)$ . We also compute the *reduced* PCAM,  $P'(T, \Delta_T)$ , which is a submatrix of the original PCAM,  $P$ , corresponding to the retained  $n'$  nodes.

### 4.3 Step-3: CAP using Autoregressive Models

We now have time series of  $N'_a$  attributes in the reduced PCAMs, with  $N_T$  time instances each, for the network. In the case of real-world graphs, we observe that these attributes, which are the probability of co-association values in PCAM, have constant first moments, *i.e.*, mean, and finite second moments, *i.e.*, variance. Hence, we can now assume that each of these  $N'_a$  attributes in PCAM forms a *weakly stationary* process. Autoregressive models (AR) (Box and Jenkins, 1970) and their variants are widely used with time series data for the prediction of *weakly stationary stochastic processes*.

**Data Formats of PCAMs:** Given that co-association is a symmetric relationship, the PCAM stores

**Input** : A sequence of snapshots of a dynamic sparse directed network (DSDN) in the form of sets  $\{V, E(T_1), E(T_2), \dots, E(T_{N_T})\}$   
**Input** : Moving-average window  $\Delta_T$ , Choice of data format  $F$  (i.e., *vector-format* or *independent-attribute-format*)  
**Input** : Parameters for the autoregressive model (i.e.,  $p$  for VAR for vector-format, or  $(p, q)$  for ARMA for independent-attribute-format)  
**Output**: Probability of Co-association Matrix (PCAM) of significant subnetwork  $P'(N_T + 1, \Delta_T)$  (i.e., reduced PCAM)

```

// Step-1
for method M in ECD (an ensemble of community detection algorithms) do
  for  $1 \leq T \leq N_T$  do
    | A community set  $C(M) \leftarrow \text{Implement}(M, \{V, E(T)\})$ 
    | Compute the CAM,  $D(T)$ , from  $C$ , using Equation 1
  end
  for  $\Delta_T \leq T \leq N_T$  do
    | Compute the PCAM,  $P(T, \Delta_T)$ , using Equation 2
    | for  $1 \leq i \leq n$  do
    | | Compute  $p_i(T, \Delta_T)$  using Equation 3 // Likelihood of a node to be co-associated
    | end
  end
end
end
Select optimal CD method  $M_{\text{opt}}$  based on quality of  $C(M)$ , cardinality of  $\|C\|$  size of communities

// Step-2
for  $1 \leq i \leq n$  do
  | Compute  $H_i(\Delta_T)$  using  $p_i$  from  $M^{\text{opt}}$ , using Equation 4
end
Sort  $H_i$  for all nodes and determine transition point as threshold  $\tau_h$ 
 $V^* = \{\}$  // Node set of the node-filtered network
for  $1 \leq i \leq n$  do
  | if  $H_i < \tau_h$  then
  | |  $V^* \leftarrow V^* \cup \{i\}$ 
  | end
end
for  $\Delta_T \leq T \leq N_T$  do
  |  $P'(T, \Delta_T) \leftarrow$  Submatrix of  $P(T, \Delta_T)$  for  $\{V^*, E(T - \Delta_T), E(T - \Delta_T + 1), \dots, E(T)\}$  // Reduced PCAM
end

// Step-3
if F is (vector-format) then
  for  $\Delta_T \leq T \leq N_T$  do
    |  $v(T) \leftarrow$  half-vectorization of  $P'(T, \Delta_T)$ 
  end
   $v(N_T + 1) \leftarrow \text{Implement}(\text{VAR}(p), \{v(\Delta_T), v(\Delta_T + 1), \dots, v(N_T)\})$ , using Equation 5 // Predict for the reduced PCAM
end
else if F is (independent-attribute-format) then
   $v(N_T + 1) \leftarrow []$ 
  for  $1 \leq i \leq \|V^*\|$  do
    | for  $\Delta_T \leq T \leq N_T$  do
    | | Compute  $p_i(T, \Delta_T)$  from  $P'(T, \Delta_T)$  using Equation 3
    | end
    |  $v_i(N_T + 1) \leftarrow \text{Implement}(\text{AR}(p, q), \{p_i(\Delta_T, \Delta_T), p_i(\Delta_T + 1, \Delta_T), \dots, p_i(N_T, \Delta_T)\})$ , using Equation 6 // Predict for each node
    |  $v(N_T + 1) \leftarrow \text{Append}(v(N_T + 1), v_i(N_T + 1))$ 
  end
end
 $P'(N_T + 1, \Delta_T) \leftarrow \text{Reverse-process of half-vectorization}(v(N_T + 1))$ 

```

Algorithm 1: The complete algorithm of CAP-DSDN for DSDNs for prediction of co-association of nodes in a subnetwork with persistent community behavior.

$N_a = \frac{n(n-1)}{2}$  unique pairwise relationships in a network of  $n$  nodes. We propose to use these co-association values as *attributes* in a data model for the prediction of community structure using the autoregressive models. This leads to two possibilities of using the attributes from the PCAM: (i) in the form of a vector, thus modeling a time series of  $N_a$ -long vector, or (ii) as independent attributes, thus, getting  $N_a$  separate time series. We use the upper or the lower triangular part of the PCAM, without the diagonal for generating (i) and (ii). Thus, we use *half-vectorization* of PCAM for (i).

**Prediction using Autoregressive Models:** Here, we choose two such models to suit the aforementioned data formats, namely, (i) the vector auto-regressive (VAR) model (Sims, 1980) for the vector format of the attributes, and (ii) the auto-regressive-moving-average (ARMA) model (Box and Jenkins, 1970) for the format of the independent attributes.

In the VAR model, for a vector  $y$  of length  $k$ , constants vector  $c$ ,  $k \times k$  matrices as coefficients  $A_i$ , a vector  $\varepsilon$  as error term, and  $p$  as the order of auto-regressive model, which is the number of time-lags, the predicted value is given as:

$$y(T) = c + \sum_{i=1}^p A_i y(T-i) + \varepsilon(T). \quad (5)$$

Since ( $N'_a \gg N_T$ ), we use low values of  $p$ , i.e.,  $p = 1, 2, 3$ . Hence, we use VAR(1), VAR(2), and VAR(3) models for our case study. Determining the optimal choice of  $p$  values using the minimization of statistics such as Akaike (AIC), Schwarz-Bayesian (BIC), etc. is in the scope of future work.

Using both AR and moving-average (MA) models together addresses a generalized structure. If we treat the  $N'_a$  attributes independently, then we can use each of their time series in an ARMA model for predictive analysis. An ARMA( $p, q$ ) process has two parameters –  $p$  is the order of the autoregressive model, and  $q$  is the order of the MA, i.e, moving average part), which gives the number of error terms considered. For time series (scalar) values  $y$  at time instance  $T$ , constant value  $c$ , coefficients of AR model  $\phi$ , coefficients of MA model  $\theta$ , and error term  $\varepsilon(T)$ ,

$$y(T) = c + \sum_{i=1}^p \phi_i y(T-i) + \sum_{i=1}^q \theta_i \varepsilon(T-i). \quad (6)$$

Since ( $N'_a \gg N_T$ ), we use low values of  $q$  also. Thus, in our case study, we use  $p = 1, 2, 3$  and  $q = 1, 2$  in an ARMA( $p, q$ ) process. Thus, we implement six ARMA( $p, q$ ) models with the selected ( $p, q$ ).

Using the predicted values of the elements of the reduced PCAM,  $P'$ , we reconstruct the matrix. The complete step-by-step procedure of CAP-DSDN is as given in Algorithm 1.

## 4.4 Prediction Evaluation

Given the absence of ground truth, we use the time series data for ( $N_T - 3$ ) time instances for our analysis to predict the remaining three time instances. Currently, the value of *three* is conservatively chosen to indicate short-term prediction and assuming that most of the DSDNs have more than three snapshots.

We compare our predicted co-association values with those values computed directly from the data of these time instances for validation. For comparison, we use the metrics conventionally used in clustering algorithms, especially in the absence of ground truth. We use the *Normalized Mutual Information Score* (NMI) (Studholme et al., 1998) and *Rand Index* (RI) (Rand, 1971) here.

NMI is a measure of the similarity between two label assignments of the same data, indicating mutual agreement of labels between the assignments. NMI values range from 0 to 1, implying the strength of the agreement. While the bounded values of NMI are an advantage for comparisons, NMI not adjusting for chance is a disadvantage for our case study. For two label assignments,  $U$  and  $V$ , with  $L$  and  $M$  classes, respectively, mutual information (MI) and NMI are computed, for  $N$  objects using entropy measure  $H$ , as:

$$H(U) = \sum_{i=1}^{|L|} P(i) \log(P(i));$$

$$H(V) = \sum_{j=1}^{|M|} P'(j) \log(P'(j)),$$

where the probabilities  $P(i)$  and  $P'(j)$  are computed using the number of instances in  $U$  and  $V$  in the  $i^{th}$  and  $j^{th}$  classes, respectively.

$$\text{Thus, } P(i) = \frac{|Class(i)|}{N} \text{ and } P'(j) = \frac{|Class(j)|}{N}.$$

When comparing the two labeling assignments, there may be some instances with both labels  $i$  and  $j$ . Thus, the joint probability is:

$$P(i, j) = \frac{|Class(i) \cap Class(j)|}{N}.$$

$$\text{Thus, } MI(U, V) = \sum_{i=1}^{|L|} \sum_{j=1}^{|M|} P(i, j) \cdot \log\left(\frac{P(i, j)}{P(i) \cdot P'(j)}\right).$$

We normalize using the sum, i.e., the mean, as it is considered a good trade-off when considering minimum, mean, and maximum value as the normalizing factor (Kvalseth, 1987). Thus, the normalized value

$$NMI(U, V) = \frac{MI(U, V)}{\text{mean}(H(U), H(V))}.$$

We consider 0 and 1 in the (binarized) CAM as labels, thus, giving  $|L| = |M| = 2$ .

RI is another similarity measure between the actual community distribution and the predicted community distribution by considering all pairs of objects, and by counting the pairs that are assigned in the same or different clusters in the predicted and true clusterings. RI is the ratio of the number of common pairs

to the total number of pairs. We use the unadjusted RI, bounded in  $[0,1]$ , as it provides the accuracy of element pair labeling as given by the clustering.

## 4.5 Implementation

We have used Python for implementing our proposed work. `CDlib` (Rossetti et al., 2019) has been used for community detection algorithms and metrics. The time series regression models VAR and ARMA have been implemented using `statsmodels` (Seabold and Perktold, 2010). The validation for prediction using the metrics for clustering has been implemented using `scikit-learn` (Pedregosa et al., 2011). Shannon entropy has been computed using `scipy.stats` (Virtanen et al., 2020), using the default logarithm base  $e$ , *i.e.*, natural logarithm.

## 5 CASE STUDY: EXPERIMENTS & RESULTS

In this section, we present the results of CAP-DSDN (Figure 1) on a case study of international refugee migration over an extended period.

**International Refugee Migration Flow:** We analyze the DSDN in a specific case study of international refugee migration flow between countries. The dataset, obtained from the United Nations Human Rights Commissioner (UNHCR)<sup>2</sup>. This publicly available dataset has year-wise records of migrant count from origin to destination (or asylum) countries, which are the flow values. While the refugee data in the UNHCR database is available from the year 1951, the count of asylum seekers was first available in 2000. Hence, we use the annual data starting in 2000 and thus, focus on the time period during 2000-2018. In this time period, there are 208 countries of origin and 186 countries of asylum. After pruning nodes that have only zero-weighted edges for all the snapshots, we reduce the node-set to 190 countries. Thus, our DSDN has 190 nodes for 19 snapshots.

Given the absence of ground truth, we use 2000-2015 data to predict the PCAM for 2016-2018 of the significant subnetwork, and the predicted values are compared against the computed values from the original data for validation.

**Selection of CD Algorithm:** The evaluation results of the three selected community detection algorithms are reported in Table 1 for a representative year, 2018,

<sup>2</sup>Dataset: <https://www.unhcr.org/refugee-statistics/download/>

which is the last year. For the link (LM) modularity, SLPA and MODN show more similar values and IMAP has a relatively lower value. For Z-Modularity (ZM), MODN performs better than IMAP and SLPA. The modularity values closer to zero indicate a single large community (Fortunato, 2010), and higher positive values, but less than one, indicate better partitioning. The LM values for the three algorithms may be explained by the community characteristics in the year 2018 (Figure 2, (i)-(ii)). We observe that SLPA gives the highest count of communities whereas IMAP gives the lowest, but all three gives similarly sized largest community. Thus we observe that IMAP has the lowest variation in community sizes, and SLPA tends to have several smaller communities, indicating a higher degree of fragmentation.

Since ZM is designed to address the issue of resolution limit, we observe that MODN with a considerable number of communities, and with moderate variation in community sizes, performs well. The community characteristics in Figure 2 also explain the relatively high values of IMAP for Internal Edge Density (IED), Average Internal Degree (AID), and Cut Ratio (CR) metrics, indicating the best performance by IMAP. Higher values of these metrics imply better communities. SLPA has a distinct advantage in the case of networks with overlapping communities (Xie et al., 2011). We observe that SLPA does not perform as well as IMAP and MODN, with respect to our chosen metrics, as our case study does not have any relevance for overlapping communities.

Overall, we observe from Table 1 that there is no single CD algorithm that distinctively or consistently performs the best, with respect to our chosen metrics. This can be explained by the known observation that these CD algorithms detect a large number of small and connected *whisker*-like communities and a large core with several intermingled communities. Using the community structure characteristics shown in Figure 2 (i)-(ii), we conclude that IMAP performs the best as it demonstrates the community structure with a large core (Figure 2 (ii)). Thus, IMAP is an appropriate choice for community detection and prediction of international refugee migration flow in our case study, as demonstrated in (Table 1 and Figure 2). It must be noted that algorithms that disregard the edge directionality information, *e.g.*, MODN, are not considered to be accurate (Agrete et al., 2016). Hence, even though MODN gives a moderate performance, we have disregarded MODN here. With respect to time complexity, SLPA is the fastest, followed by IMAP closely, but MODN has the worst performance (Agrete et al., 2016). Since time complexity is also a critical factor for the choice of CD



Table 1: Comparing communities in the international refugee migration flow in the year **2018**, in 190 countries, using different algorithms, evaluated by different metrics.

Community Detection Algorithm	LM	IED	AID	CR	ZM
SLPA	<b>0.028</b>	0.019	0.643	0.004	0.108
MODN	<b>0.028</b>	0.009	1.093	0.005	<b>0.451</b>
IMAP	0.019	<b>0.114</b>	<b>3.647</b>	<b>0.048</b>	0.207

SLPA: speaker-listener label propagation algorithm; MODN: modularity optimization in a directed network; IMAP: Infomap algorithm. LM: link modularity; IED: internal edge density; AID: average internal degree; CR: cut ratio; ERM: Erdős-Rényi modularity; ZM: Z-modularity.

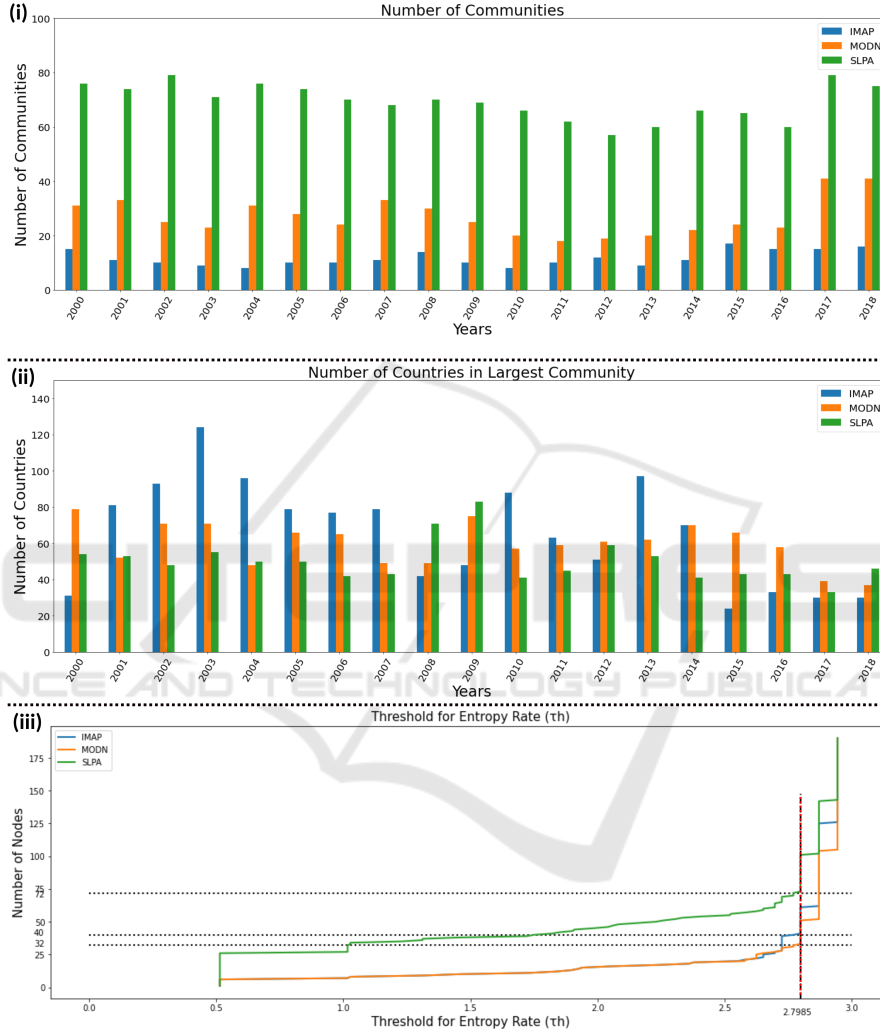


Figure 2: For the selected CD algorithms, (i)-(ii) characteristics of CD outcomes, and (iii) number of nodes retained for different thresholds for determining entropy rate  $\tau_h$  (red dotted line), for the international refugee migration flow in 190 countries (nodes of the DSDN).

algorithm, IMAP is the optimal choice here.

**Node-filtering the Network:** Each CD algorithm can independently have its own  $\tau_h$ . But, in this case study, we observe that all three algorithms have the same  $\tau_h = 2.799$  as the transition point for entropy rate in their CD outcomes (Figure 2, (iii)). Using this value as the threshold, we get node-filtered networks of size

$n'$ , i.e., 72, 32, and 40 nodes, in the case of SLPA, MODN, and IMAP, respectively. This indicates that IMAP is a conservative choice.

**Time Series Modeling and Prediction:** A summary of the experiments for the IMAP algorithm (for both, VAR and ARMA) for the network sizes upon filtering, are given in Table 2. For each VAR experiment,

Table 2: Comparison of the predicted PCAMs using autoregressive models, *i.e.*, VAR( $p$ ) and ARMA( $p,1$ ) models, for communities detected using Infomap algorithm (IMAP), in the international refugee migration network with  $n = 190$  nodes, giving  $n'$  nodes after node-filtering the DSDN using threshold  $\tau_h$ , in different prediction years (Pred. Yr.).

Pred. Yr. → Metric ↓	2016			2017			2018		
<b>VAR(<math>p</math>)</b>	$p = 1$	$p = 2$	$p = 3$	$p = 1$	$p = 2$	$p = 3$	$p = 1$	$p = 2$	$p = 3$
	$\tau_h = 2.799, n' = 40$ , Using IMAP								
NMI	0.000	0.000	0.064	0.000	0.000	0.000	0.000	0.000	0.000
Rand-Index	0.943	0.943	0.945	0.982	0.982	0.980	<b>0.992</b>	<b>0.992</b>	0.990
<b>ARMA(<math>p,1</math>)</b>	$p = 1,$	$p = 2,$	$p = 3,$	$p = 1,$	$p = 2,$	$p = 3,$	$p = 1,$	$p = 2,$	$p = 3,$
	$\tau_h = 2.799, n' = 40$ , Using IMAP								
NMI	0.039	0.039	0.039	0.015	0.015	0.015	0.008	0.008	0.008
Rand-Index	0.057	0.057	0.057	0.018	0.018	0.018	0.008	0.008	0.008

NMI: normalized mutual information; VAR: vector auto-regression; ARMA: auto-regressive moving average.

the time series of the vector  $v$  of size  $N'_a = \frac{n'(n'-1)}{2}$ , as the vector is obtained from the half vectorization of the reduced PCAM (of  $n'$  nodes), after discarding the zeros on the diagonal. On the other hand, ARMA is implemented separately for the time series of  $N'_a$  different elements of  $v$ , used in the VAR model. We make three major observations.

Firstly, the RI gives more variation in the results than the NMI values, as the latter is a more stringent validation metric than the former. This is because RI compares pairwise similarities in the binary values in the predicted and the original CAMs, whereas NMI directly compares the matrix values in the CAMs.

Secondly, the VAR model gives better results than the ARMA model, which can be explained by the consideration of interdependence between the attributes in the former than in the latter. Also, the disparity  $N'_a \gg N_T$ , for  $N_T$  time instances, plays a role in over-fitting solutions for the ARMA model.

Thirdly, the AR parameter  $p$  value does not have any impact on improving the ARMA model.  $p = 1, 2$  show best results for the VAR( $p$ ) model. Given the disparity,  $p = 1$  may be considered the most conservative value for the VAR( $p$ ). We also found that the MA parameter  $q = 2$  showed the same results as  $q = 1$ , in the ARMA( $p, q$ ) model. Hence, we consider only AR( $p, q$ ) only for  $q = 1$  in our experiments.

Overall, IMAP gives the best result for VAR(1) for the year 2018. Given the political volatility of international refugee migration, short-term predictions are preferred over long-term ones. Thus, we conclude that CAP-DSDN can be effectively used in international refugee migration flow analysis for conservative predictions of the community structure in the significant subnetwork over *three years*.

As an example of co-association available from the dataset, the communities in the network in the year 2015 show that the USA and Mexico are in the same community. Based on the trend of the re-

duced number of migrations due to geopolitical circumstances over the years, our model predicts their co-association to be zero in 2018. The actual co-association value matches the same and correlates with the fact that the proportion of the Mexican-born population in the USA declined from 28% to 26% in this duration (Krogstad and Radford, 2017).

Another example is that of Australia, where the migration rates have continued to decline since 2004. The CAM in 2015 shows that Australia belongs to a community of 65 countries. The predicted CAM shows that the community behavior has fallen steeply, and Australia belongs to a community with 37 countries, which is reasonably close to the actual value of 29 (United Nations, Dept. of Econ. & Soc. Affairs, Population Div., 2015).

## 6 CONCLUSIONS

It is important to note that in the previous literature while determining communities in DSDNs, the community of nodes is seen as an entity rather than its pairwise relationships. Instead of performing a time series analysis of the network itself or its communities, we have shifted our focus to the inter-relationships between the network nodes which is a novelty of CAP-DSDN. In this node-centric approach, we use the relationship of co-association in a community, which we use for predictive analysis. We use the co-association matrices (CAM) to represent these relationships while representing the discovered communities of nodes indirectly. When using a time window, the moving average smoothing of the CAM gives a likelihood value for the co-association relationship, which is the PCAM. Furthermore, we use the elements of PCAM as attributes for the predictive model for a time series dataset. Lastly, the outcome of our study is in predicting the co-association value at a

future date, thus indirectly predicting the community structure in a significant subnetwork. This significant subnetwork retains only the nodes with a strong community forming tendency over time, determined using our novel entropy rate metric. Overall, our results in the case study of the international refugee migration network demonstrate that the effectiveness of our proposed method depends strongly on the completeness of the time series data.

There are limitations in our work stemming from the data quality and availability, concerning the migration flow datasets. Finding datasets outside of migration flow is non-trivial, given the nuanced properties expected of the dataset, *i.e.*, directed networks, sparse, and with time series. Further research can be pursued for migration flow data analysis itself in improving the data quality using imputation and other methods appropriate for the data.

## ACKNOWLEDGEMENTS

The authors acknowledge the support of the IIIT Bangalore and the IIT Kharagpur summer internship program for conducting this work. The authors are grateful to the anonymous reviewers whose suggestions have improved this paper. This publication is supported by the grant by the Science and Engineering Research Board (SERB), Government of India, under the Mathematical Research Impact Support (MATRICS). The authors are thankful to the help provided by members of the Graphics-Visualization-Computing Lab.

## REFERENCES

- Agreste, S., De Meo, P., Fiumara, G., and *et al.* (2016). An empirical comparison of algorithms to find communities in directed graphs and their application in web data analytics. *IEEE Transactions on Big Data*, 3(3):289–306.
- Bongiorno, C., Zino, L., and Rizzo, A. (2019). A novel framework for community modeling and characterization in directed temporal networks. *Appl. Net. Sc.*, 4(1):1–25.
- Box, G. and Jenkins, G. (1970). *Time Series Analysis: Forecasting and Control*. Holden-Day, San Francisco.
- Cai, D., Campbell, T., and Broderick, T. (2016). Edge-exchangeable graphs and sparsity. *Advances in Neural Info. Processing Sys.*, 29.
- Cover, T. M. and Thomas, J. A. (2006). *Elements of Information Theory (Wiley Series in Telecommunications and Signal Processing)*. Wiley-Intersc.
- Fortunato, S. (2010). Community Detection in Graphs. *Phys. Reports*, 486(3-5):75–174.
- Krogstad, J. M. and Radford, J. (2017). Key facts about refugees to the US. *Pew Rsrch. Cntr.*, 30.
- Krzakala, F., Moore, C., Mossel, E., Neeman, J., Sly, A., Zdeborová, L., and Zhang, P. (2013). Spectral redemption in clustering sparse networks. *Proceedings of the National Academy of Sciences*, 110(52):20935–20940.
- Kvalseth, T. O. (1987). Entropy and correlation: Some comments. *IEEE Transactions on Systems, Man, and Cybernetics*, 17(3):517–519.
- Leicht, E. A. and Newman, M. E. (2008). Community structure in directed networks. *Phys. Rev. Letters*, 100(11):118703.
- Malliaros, F. D. and Vazirgiannis, M. (2013). Clustering and community detection in directed networks: A survey. *Phys. Reports*, 533(4):95–142.
- Martin, S., Morărescu, I.-C., and Nešić, D. (2016). Time scale modeling for consensus in sparse directed networks with time-varying topologies. In *2016 IEEE 55th Conference on Decision and Control (CDC)*, pages 7–12. IEEE.
- Mirshahvalad, A., Lindholm, J., Derlen, M., and Rosvall, M. (2012). Significant communities in large sparse networks. *PLoS one*, 7(3):e33721.
- Miyachi, A. and Kawase, Y. (2016). Z-score-based modularity for community detection in networks. *PLoS one*, 11(1):e0147805.
- Neumayer, E. (2005). Bogus refugees? The determinants of asylum migration to Western Europe. *International studies quarterly*, 49(3):389–409.
- Nicosia, V., Mangioni, G., Carchiolo, V., and Malgeri, M. (2009). Extending the definition of modularity to directed graphs with overlapping communities. *Jrnl. of Stat. Mech.: Theory and Experiment*, 2009(03):P03024.
- Pedregosa, F., Varoquaux, G., Gramfort, A., and *et al.* (2011). Scikit-learn: Machine Learning in Python. *Journal of Machine Learning Research*, 12:2825–2830.
- Pons, P. and Latapy, M. (2006). Computing communities in large networks using random walks. *Journal of Graph Algorithms and Applications*, 10(2):191–218.
- Radicchi, F., Castellano, C., Cecconi, F., Loreto, V., and Parisi, D. (2004). Defining and identifying communities in networks. *PNAS*, 101(9):2658–2663.
- Rand, W. M. (1971). Objective criteria for the evaluation of clustering methods. *Journal of the American Statistical Association*, 66(336):846–850.
- Rossetti, G. and Cazabet, R. (2018). Community discovery in dynamic networks: A survey. *ACM Computing Surveys (CSUR)*, 51(2):1–37.
- Rossetti, G., Milli, L., and Cazabet, R. (2019). CDLIB: A Python Library to Extract, Compare and Evaluate Communities from Complex Networks. *Applied Network Science*, 4(1):1–26.
- Rosvall, M. and Bergstrom, C. T. (2008). Maps of random walks on complex networks reveal community structure. *PNAS*, 105(4):1118–1123.

- Seabold, S. and Perktold, J. (2010). statsmodels: Econometric and statistical modeling with Python. In *9th Python in Science Conference*.
- Sims, C. A. (1980). Macroeconomics and reality. *Econometrica: journal of the Econometric Society*, pages 1–48.
- Singh, A. and Humphries, M. D. (2015). Finding communities in sparse networks. *Scientific reports*, 5(1):1–7.
- Stein, S. and Leng, C. (2021). A Sparse Random Graph Model for Sparse Directed Networks. *arXiv preprint arXiv:2108.09504*.
- Studholme, C., Hawkes, D. J., and Hill, D. L. G. (1998). Normalized entropy measure for multimodality image alignment. In *Medical Imaging 1998: Image Processing*, volume 3338, pages 132–143. Intl. Society for Optics & Photonics.
- Suleimenova, D., Bell, D., and Groen, D. (2017). A generalized simulation development approach for predicting refugee destinations. *Scientific reports*, 7(1):1–13.
- United Nations, Dept. of Econ. & Soc. Affairs, Population Div. (2015). *International Migration Flows to and from Selected Countries: The 2015 Revision*.
- Virtanen, P., Gommers, R., Oliphant, T. E., et al., and SciPy 1.0 Contributors (2020). SciPy 1.0: Fundamental Algorithms for Scientific Computing in Python. *Nature Methods*, 17:261–272.
- Wang, B., Gao, L., and Gao, Y. (2012). Control range: a controllability-based index for node significance in directed networks. *Jrnl. of Stat. Mech.: Theory and Experiment*, 2012(04):P04011.
- Xie, J., Szymanski, B. K., and Liu, X. (2011). SLPA: Uncovering overlapping communities in social networks via a speaker-listener interaction dynamic process. In *IEEE 11th Intl. Conf. on Data Mining Workshops*, pages 344–349. IEEE.